2D Semi-Analytical Modeling of Eddy Currents in Segmented Structures

C.H.H.M. Custers, T.T. Overboom, J.W. Jansen, and E.A. Lomonova

Department of Electrical Engineering, Eindhoven University of Technology, Eindhoven, The Netherlands

The paper concerns the semi-analytical modeling of eddy currents in segmented structures of electromagnetic devices. A Fourier series is used to describe the spatial distribution of the conductivity and included in the magnetic field solutions. By incorporating multiple time harmonics in the solution, transient behavior of forces due to eddy currents can be obtained. To validate the developed method, it is applied to a coreless linear motor and compared to finite element results. The eddy currents in segmented conducting structures of motors, such as permanent magnet arrays, can be accurately determined with this method.

Index Terms—**Eddy current, Fourier analysis, Permanent Magnet Machines, Analytical Modeling.**

I. INTRODUCTION

IN synchronous permanent magnet (PM) machines, the static field of the magnets interacts with a time varying field caused by a set of coils. Besides the intended force, also parasitic forces are produced, for instance due to eddy currents induced in non-laminated conducting parts of the machine, such as the magnets. These currents and their associated force and losses depend on the structure of the magnets and can be reduced by segmentation [1]. Hence, to accurately predict the eddy current behavior in the magnets, their finite dimensions and segmentation has to be taken into account.

The 2D Fourier analysis technique [2], [3], is a fast alternative for finite element analysis for the design and analysis of electromagnetic devices. With this semi-analytical technique, eddy currents and their reaction field can be modeled. A limitation of this method as described in [2], [4] is that the eddy currents are only calculated in a infinitely long electrically conducting slab with homogeneous material properties, and as a result, segmentation is not taken into account. To overcome this limitation, in [5] the eddy currents in a conducting plate with finite length are approximated with the method of images. However, for problems in which the conducting part is smaller than the source of the magnetic field the results are inaccurate.

In this paper, the Rigorous Coupled Wave Analysis (RCWA) technique [6] is applied to 2D quasi-static magnetic field modeling of motor topologies with a variable conductivity in the Cartesian domain. In [6], the diffraction of a high-frequent electromagnetic wave by a planar grating with a position dependent permittivity and permeability is modeled. With this technique, inhomogeneous material properties are included in the solution of electromagnetic field quantities. By incorporating a position dependent conductivity function in the Fourier based field analysis, eddy currents in segmented parts are modeled. The developed method is applied to a coreless motor model of which the top half of a periodic section is shown in Fig. 1. The back-iron is assumed to be infinitely permeable and nonconductive because the focus of the paper is on the eddy currents induced in the segmented region.

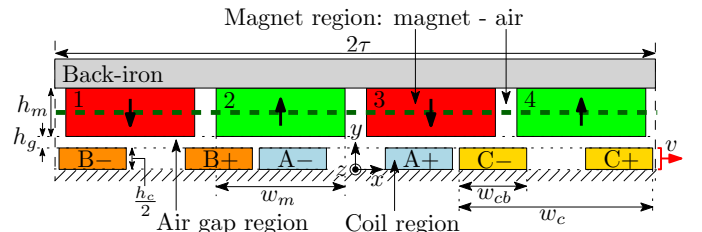Corresponding author: c.h.h.m.custers@tue.nl

Fig. 1. Top half geometric model of a periodic section of a linear coreless motor.

II. MAGNETIC FIELD MODELING

The model of the coreless motor of Fig. 1 is divided into three horizontal regions, respectively the magnet region, air gap region and coil region. To obtain the solutions of the magnetic field quantities, the vector potential formulation is used. The magnetic vector potential $\vec{A}$ is defined as $\vec{B} = \nabla \times \vec{A}$, where $\vec{B}$ is the magnetic flux density. Because a two-dimensional problem is treated, the vector potential is reduced to the z-component. Based on Maxwell's equations and the constitutive relations, the Poisson equation is derived for nonconducting regions

$$\frac{\partial^2 A_z}{\partial x^2} + \frac{\partial^2 A_z}{\partial y^2} = -\mu_0 \frac{\partial M_y}{\partial x} - \mu_0 \mu_r J_z^{ext}, \qquad (1)$$

where μ_0 is the permeability of vacuum and μ_r is the relative permeability. M_y is the remanent magnetization and J_z^{ext} is an externally imposed current density.

In the magnet region, eddy currents are induced, which can be obtained from the vector potential by

$$J_z^{eddy} = -\sigma(x) \frac{\partial A_z}{\partial t}, \qquad (2)$$

where $\sigma(x)$ describes the position dependent conductivity of the magnet array. Generally, the vector potential of a conducting region has to satisfy the diffusion equation

$$\frac{\partial^2 A_z}{\partial x^2} + \frac{\partial^2 A_z}{\partial y^2} = -\mu_0 \frac{\partial M_y}{\partial x} + \mu_0 \mu_r \sigma(x) \frac{\partial A_z}{\partial t}. \qquad (3)$$

III. SEMI-ANALYTICAL SOLUTION

The magnetic field solutions are expressed in terms of Fourier series. The model is assumed to be periodical in the

x-direction. As a result, the x-dependent solution is described by a complex Fourier series. To model the movement of the coil array, also the time dependent solution is described by a Fourier series. Because there is no correlation between the different time harmonics the principle of superposition is applicable. As a consequence, the vector potential solution can be determined for each time harmonic separately and the results can be superimposed. The solution to the vector potential is found by applying the method of separation of variables and has the following general form with a homogeneous and particular solution respectively

$$A_z(x,y,t) =$$
$$\sum_{m=-\infty}^{\infty} \sum_{n=-\infty}^{\infty} \left(P_{m,n}(x,y,t) + Y_{m,n}(y)\ e^{j(k_n x + \omega_m t)} \right). \quad (4)$$

The spatial frequency, k_n, is defined as $k_n = \frac{n\pi}{\tau}$, where τ is half of the periodic width of the model and $\omega_m = \frac{m2\pi}{T}$, where T is the time period. The y-dependent solution $Y_{m,n}(y)$ is equal to

$$Y_{m,n}(y) = a_{m,n}\ e^{\sqrt{\lambda_{m,n}}y} + b_{m,n}\ e^{-\sqrt{\lambda_{m,n}}y}, \quad (5)$$

where $a_{m,n}$ and $b_{m,n}$ are unknown coefficients for each harmonic which will be determined by applying boundary conditions between the regions. The eigenvalues $\lambda_{m,n}$ of the y-dependent solution are derived in section III-B and III-C. $P_{m,n}(x,y,t)$ in (4) is the particular solution that is related to the source terms and will be derived in the following section.

A. Particular solution

For the magnet region the following holds for the particular solution

$$P_{0,n}(x) = \begin{cases} \mu_0 \frac{1}{k_n} M_{y_{0,n}}\ e^{jk_n x} & \text{for } |n| > 0, \\ 0 & \text{for } n = 0, \end{cases} \quad (6)$$

where $M_{y_{0,n}}$ are the Fourier coefficients describing the spatial distribution of the magnetization which does not depend on time. For the coil region with the source current density the following holds

$$P_{m,n}(x,y,t) = \begin{cases} \mu_0 \mu_r \frac{1}{k_n^2} J_{z_{m,n}}^{ext} e^{j(k_n x + \omega_m t)} & \text{for } |n| > 0, \\ -\mu_0 \mu_r \frac{1}{2} J_{z_{m,n}}^{ext} y^2 e^{j(k_n x + \omega_m t)} & \text{for } n = 0. \end{cases} \quad (7)$$

where $J_{z_{m,n}}^{ext}$ are the Fourier coefficients that describe the spatial and time distribution of the externally imposed current density. The three-phase current density in the coil array, described by $J_{z_{m,n}}^{ext}$, is sinusoidal and synchronously commutated for maximum propulsion force. This means that the frequency of the current is equal to $f = \frac{v}{\tau}$, where v is the speed of the coil array. The time varying behavior of the current density is written as the complex form of a cosine function

$$J_{ph}(t) = \hat{J} \frac{1}{2} \left(e^{j(2\pi \frac{v}{\tau} t + \theta_{ph})} + e^{-j(2\pi \frac{v}{\tau} t + \theta_{ph})} \right), \quad (8)$$
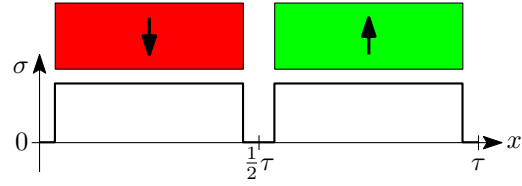

Fig. 2. Varying conductivity as a function of position in the magnet region.

where $\hat{J}$ is the peak current density, ph denotes the phase and $\theta_A = 0$, $\theta_B = -\frac{2\pi}{3}$ and $\theta_C = \frac{2\pi}{3}$. The coefficients $J_{z,ph_{m,n}}$ of phase ph are calculated by performing the integral

$$J_{z,ph_{m,n}} = \hat{J} K_{ph_n} \frac{1}{2T} \int_0^T$$
$$\left(e^{j(2\pi \frac{v}{\tau} t + \theta_{ph})} + e^{-j(2\pi \frac{v}{\tau} t + \theta_{ph})} \right) e^{-jk_n vt} e^{-jw_m t} dt, \quad (9)$$

where K_{ph_n} are the coefficients of the spatial distribution of the current density of phase ph. The coefficients $J_{z_{m,n}}^{ext}$ are obtained by $J_{z_{m,n}}^{ext} = J_{z,A_{m,n}} + J_{z,B_{m,n}} + J_{z,C_{m,n}}$.

B. Homogeneous solution for nonconducting regions

For the nonconducting regions the eigenvalues $\lambda_{m,n}$ are determined by

$$\lambda_{m,n} = k_n^2. \quad (10)$$

In the nonconducting region, the eigenvalue of harmonic number n depends only on spatial frequency k_n. This means that the spatial harmonics are uncorrelated. The matrix representation of (10) is given by

$$\mathbf{\Lambda}_m = \mathbf{K}^2, \quad (11)$$

where $\mathbf{K}$ is a diagonal matrix containing the spatial frequencies k. The matrix $\mathbf{\Lambda}_m$ is also diagonal and contains the eigenvalues λ_m of time harmonic m.

C. Homogeneous solution for conducting regions

The conductivity σ in the magnet region varies as function of position. A Fourier series is introduced that represents the spatial distribution of σ inside the region

$$\sigma(x) = \sum_{n=-\infty}^{\infty} \psi_n\ e^{jk_n x}. \quad (12)$$

The coefficients ψ_n in (12) are obtained by calculating the Fourier transform of the function shown in Fig. 2. For this function it holds that $\sigma > 0$ for positions where conductive material is present and $\sigma = 0$ for positions where air is located. Up on substituting (12) and homogeneous solution of (4) in the diffusion equation of (3) and performing the derivatives, the following is obtained

$$\sum_{n=-\infty}^{\infty} \lambda_{m,n} Y_{m,n}(y) e^{jk_n x} = \sum_{n=-\infty}^{\infty} k_n^2 Y_{m,n}(y) e^{jk_n x} +$$
$$j\omega_m \mu_0 \mu_r \left(\sum_{n=-\infty}^{\infty} \psi_n e^{jk_n x} \right) \left(\sum_{n=-\infty}^{\infty} Y_{m,n}(y) e^{jk_n x} \right). \quad (13)$$

This equation contains the product of two series with the same spatial frequencies. A new series with the same spatial
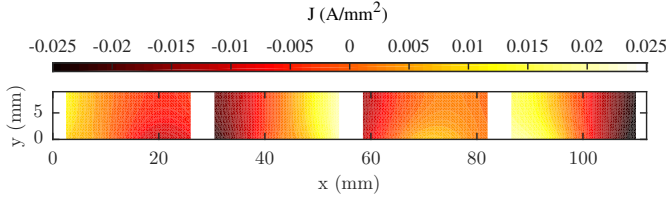
Fig. 3. Eddy current density in the magnets calculated by FEA.

TABLE I
DIMENSIONS OF THE CORELESS MOTOR

Dimension	Symbol	Value	Unit
Half periodic width	τ	56.0	mm
Air gap height	h_g	1.0	mm
Magnet width	w_m	24.0	mm
Magnet height	h_m	9.0	mm
Coil width	w_c	36.0	mm
Conductor bundle width	w_{cb}	12.5	mm
Coil height	h_c	8.0	mm

frequencies can be calculated, according to Laurent's multiplication rule [7]

$$j\omega_m\mu_0\mu_r \left(\sum_{n=-\infty}^{\infty} \psi_n e^{jk_n x} \right) \left(\sum_{n=-\infty}^{\infty} Y_{m,n} e^{jk_n x} \right) = \\ j\omega_m\mu_0\mu_r \sum_{n=-\infty}^{\infty} \sum_{q=-\infty}^{\infty} \psi_q \, Y_{m,n-q} \, e^{jk_n x}. \tag{14}$$

This multiplication can be written in matrix form

$$\boldsymbol{\Psi} \, \boldsymbol{y}_m, \tag{15}$$

where $\boldsymbol{y}_m$ is a vector containing the coefficients of the y-dependent solution. The matrix $\boldsymbol{\Psi}$ is a Toeplitz matrix containing the coefficients of $\sigma(x)$. Using Laurent's multiplication rule, the solution of $\boldsymbol{\Lambda}_m$ is given by

$$\boldsymbol{\Lambda}_m = \boldsymbol{K}^2 + \mu_0\mu_r j\omega_m\boldsymbol{\Psi}. \tag{16}$$

Contrary to Section III-B, the eigenvalue $\lambda_{m,n}$ of harmonic number n depends on multiple spatial frequencies and a coupling of different spatial harmonics occurs. As a result, the matrix $\boldsymbol{\Lambda}_m$ is not diagonal and the eigenvalues of the y-dependent solution are not directly obtained. To determine the eigenvalues, an eigenvalue decomposition is performed on $\boldsymbol{\Lambda}_m$

$$\boldsymbol{\Lambda}_m = \boldsymbol{Q}_m\boldsymbol{\Lambda}'_m\boldsymbol{Q}_m^{-1}, \tag{17}$$

where $\boldsymbol{\Lambda}'_m$ is a diagonal matrix containing the eigenvalues and $\boldsymbol{Q}_m$ is the matrix containing the corresponding eigenvectors. After performing the decomposition, the solution of A_z is equal to

$$A_z(x,y,t) = \sum_{m=-\infty}^{\infty} \left(\sum_{n=-\infty}^{\infty} P_{m,n}(x,y,t) \right) + \\ \left(e^{j\omega_m t}\boldsymbol{Q}_m \left(\boldsymbol{E}_{\boldsymbol{y}_m}(y)\boldsymbol{a}_m + \boldsymbol{E}_{\boldsymbol{y}_m}(-y)\boldsymbol{b}_m \right) \right)^\top e^{j\boldsymbol{k}x}, \tag{18}$$

where

$$\boldsymbol{E}_{\boldsymbol{y}_m}(y) = \operatorname{diag}\left(e^{\sqrt{\boldsymbol{\lambda}'_m}y} \right). \tag{19}$$

The unknown coefficients, which are determined by applying boundary conditions between regions, are collected in vectors denoted by $\boldsymbol{a}_m$, $\boldsymbol{b}_m$. The vectors $\boldsymbol{\lambda}'_m$ and $\boldsymbol{k}$ contain the diagonal entries of $\boldsymbol{\Lambda}'_m$ and $\boldsymbol{K}$ respectively.

IV. MODEL VERIFICATION

The coreless motor of Fig. 1 is modeled to verify the developed method. Because the model is symmetric with respect to the x-axis a Neumann boundary condition is applied in the center of the coils and no forces in the y-direction are considered. The dimension of the simulated motor are listed in Table I. The force exerted on the segmented magnet

array are calculated using the Maxwell Stress tensor. To only model the eddy current force acting on the magnet array, the magnetization of the magnets is set to 0 A/m and their relative permeability μ_r is set to 1. The back-iron is assumed to be infinitely permeable and nonconductive, and therefore, it is replaced by a Neumann boundary condition.

The results of the developed semi-analytical method are compared to results obtained from a transient FE analysis performed with Cedrat Flux 2D [8]. The back-iron is also replaced by a Neumann boundary. The current density in the coils is commutated on the q-axis and has a peak value of $\hat{J} = 5$ A/mm². A second order triangular mesh is applied to the model. The mesh size throughout the entire model is equal to 0.5 mm, which results in a total number of 15826 mesh elements. Assuming that at least three mesh elements per skin depth are required for simulation of eddy currents, results of the FE analysis are accurate up to a frequency of 5.6 kHz for $\sigma = 2 \cdot 10^7$ S/m. Fig. 3 shows the eddy current distribution in the magnets at one time instant, calculated by FEA.

A. Modeling multiple conducting segments

In the model, eddy currents are induced in four separate magnets. When the conductivity function describes the conductivity of multiple segments as shown in Fig. 2, the obtained results are incorrect because the segments are modeled as if they are connected while they are in fact electrically isolated. This is illustrated by the solid line in Fig. 4, where the calculated eddy currents are shown in the center of the magnets (dashed line in Fig. 1) as a function of the position. In this steady-state simulation, the coils are stationary and excited with a frequency of 50 Hz. The sum of currents inside one magnet is not equal to 0 A. To approach the correct result, the conductivity function has to describe the conductivity of one segment only and the eddy currents are calculated for each segment separately. Afterwards the results are superimposed. This result is shown in Fig. 4 by the dashed line, which is in good agreement with the FE simulation. The error with respect to the FE analysis result is less than 1 %. The method of calculating the eddy currents in each segment separately is used in the remainder of the paper. The disadvantage of this method is that the effects of the eddy currents in the individual segments on each other are not modeled.

B. Modeling transient behavior

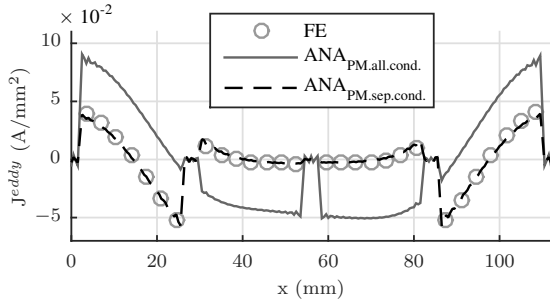To verify the transient forces during movement obtained with the developed semi-analytical model, a simulation is

Fig. 4. Eddy current density as a function of position in the center of the magnets compared to FE results. $\text{ANA}_{PM.all.cond.}$ is the result of using a conductivity function that describes the conductivity of all magnets. $\text{ANA}_{PM.sep.cond.}$ is the result of using a conductivity function that describes the magnets separately. The conductivity of the magnets is $1 \cdot 10^6$ S/m.
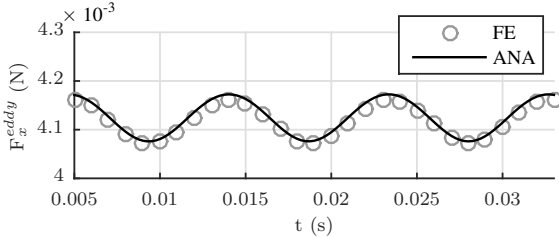

Fig. 5. Verification of obtained transient eddy current force in the x-direction.

performed in which the coil array moves in the positive x-direction with a constant speed of $v = 1$ m/s. The conductivity of the magnets is set to $1 \cdot 10^6$ S/m, which is a typical conductivity value for sintered NdFeB magnets. The results are obtained using 61 spatial harmonics and 61 time harmonics. The eddy current force is shown in Fig. 5. The error at the peak values of the force is less than 3 % with respect to the FE result.

To analyze the accuracy of the method of calculating eddy currents in individual segments and superimposing the resulting force, a transient simulation is performed at several speeds and for three values of the conductivity. Two different cases are studied. Firstly, a simulation is performed in which magnet 1 of Fig. 1 is conducting, while the other magnets are not. The mean force due to the eddy currents of both the developed semi-analytical method and FE analysis is shown in Fig. 6a. The figure shows that for all conductivity values the results are in good agreement and the maximum error with respect to the FE result is less than 4 %. Secondly, a simulation is performed in which all four magnets are conducting (Fig. 6b). For a conductivity value of $1 \cdot 10^6$ S/m, the maximum error is 2 %. However, for conductivity values higher than $1 \cdot 10^7$ S/m the error significantly increases, especially at high speeds. This is caused by the influence of the eddy current distribution in one magnet on another magnet, which is larger at high conductivity values.

V. CONCLUSION

In this paper a 2D magnetic field modeling technique has been presented that is capable of modeling the spatial distribution of the conductivity. The conductivity has been described by a Fourier series and incorporated in the solution of magnetic field quantities. With this method the eddy currents in segmented structures are modeled. The inclusion of multiple
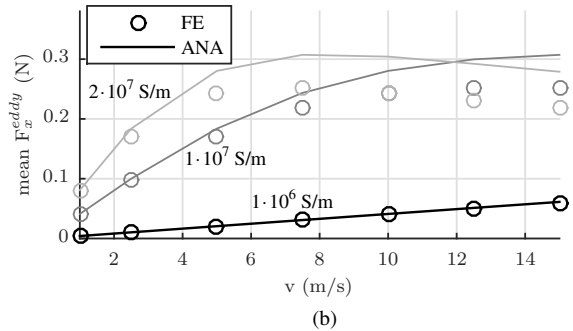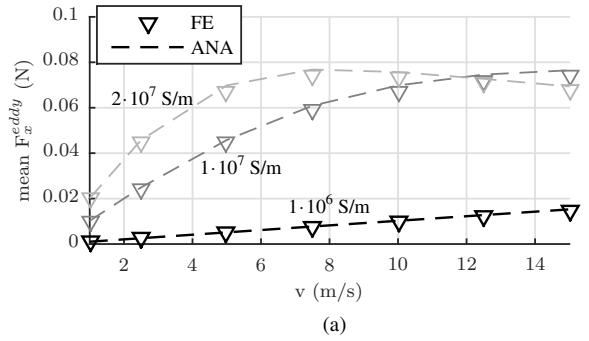

(a)

(b)

Fig. 6. Mean eddy current force versus speed for 3 different values of the conductivity. (a) Resulting force when only magnet 1 is conducting. (b) Resulting force when all magnets are conducting.

time harmonics to the solution makes it possible to model transient eddy current forces.

With the presented method it is not possible to model the spatial conductivity distribution of multiple conducting segments at once. When multiple conducting segments are considered inside a region, the conductivity of each segment has to be separately modeled and the results have to be summed. As a consequence, the effects of the eddy currents in the individual segments on each other is not modeled. However, for typical conductivity values of NdFeB magnets, accurate results (less than 3 % error with respect to FE) have been obtained with superposition.

REFERENCES

[1] K. Yamazaki, M. Shina, Y. Kanou, M. Miwa, and J. Hagiwara, "Effect of eddy current loss reduction by segmentation of magnets in synchronous motors: Difference between interior and surface types," *Magnetics, IEEE Transactions on*, vol. 45, no. 10, pp. 4756–4759, Oct 2009.

[2] K. Binns, P. Lawrenson, and C. Trowbridge, *The Analytical and Numerical Solution of Electric and Magnetic Fields*. Wiley, 1992.

[3] L. Wu, Z. Zhu, D. Staton, M. Popescu, and D. Hawkins, "Analytical model for predicting magnet loss of surface-mounted permanent magnet machines accounting for slotting effect and load," *Magnetics, IEEE Transactions on*, vol. 48, no. 1, pp. 107–117, Jan 2012.

[4] J. W. Jansen, E. A. Lomonova, and J. M. M. Rovers, "Effects of eddy currents due to a vacuum chamber wall in the airgap of a moving-magnet linear actuator," *Journal of Applied Physics*, vol. 105, no. 7, 2009.

[5] K. Pluk, T. van Beek, J. Jansen, and E. Lomonova, "Modeling and measurements on a finite rectangular conducting plate in an eddy current damper," *Industrial Electronics, IEEE Transactions on*, vol. 61, no. 8, pp. 4061–4072, Aug 2014.

[6] M. G. Moharam and T. K. Gaylord, "Rigorous coupled-wave analysis of planar-grating diffraction," *J. Opt. Soc. Am.*, vol. 71, no. 7, pp. 811–818, Jul 1981.

[7] L. Li, "Use of fourier series in the analysis of discontinuous periodic structures," *J. Opt. Soc. Am. A*, vol. 13, no. 9, pp. 1870–1876, Sep 1996.

[8] *Flux 11 User's guide*, release 11.2 ed., Cedrat Corporation, Grenoble, 2012.